A Semianalytic Radiance Model of Ocean Color

Howard R. Gordon,[1] Otis B. Brown,[2] Robert H. Evans,[2] James W. Brown,[1]
Raymond C. Smith,[3] Karen S. Baker,[4] and Dennis K. Clark[5]

A semianalytical radiance model is developed which predicts the upwelled spectral radiance at the sea surface as a function of the phytoplankton pigment concentration for Morel Case 1 waters. The model is in good agreement with experimental measurements carried out in waters which were not included in the data base used to derive it. It suggests that the observed variability in the radiance is due to variations in the backscattering of plankton and the associated detrital material. The model is extended to include other material in the water, such as dissolved organic material, referred to as yellow substances, and detached coccoliths from coccolithophorids, e.g., *Emiliana huxleyi*. Potential applications include an improved bio-optical algorithm for the retrieval of pigment concentrations from satellite imagery in the presence of interference from detached coccoliths and an improved atmospheric correction for satellite imagery. The model also serves to identify and to interpret deviations from Case 1 waters.

Introduction

The quantitative assessment of marine phytoplankton production and the role of this production for the possible storage of CO_2 in the oceans is a critical environmental and scientific problem. The oceans cover nearly three-fourths of the Earth's surface. They exhibit physical and biological variability over a wide range of space and time scales, which have led to recent development in multiplatform sampling strategies [Smith et al., 1987, and references therein]. Multiplatform (ship, buoy, aircraft, and satellite) sampling strategies allow distributions of physical and biological properties to be measured over large areas synoptically and over long time periods. These new sampling strategies rely on bio-optical models, which link ocean optical properties and in-water biological constituents for the remote (aircraft and satellite) and/or the continuous (ship and buoy) estimation of these constituents. We present here a semianalytic radiance model which predicts the upwelled spectral radiance at the sea surface as a function of the phytoplankton pigment biomass for Case 1 waters.

For analysis and interpretation of the color of the ocean, whether observed from just beneath the sea surface or at satellite altitudes, Morel and Gordon [1980] describe three approaches: (1) empirical, i.e., relying completely on statistical relationships between the upward radiance at the sea surface and the quantity of interest; (2) semiempirical, in which some modeling of the physics is introduced; and (3) analytic, in which radiative transfer models are used to extract the inherent optical properties from which the desired quantities are derived. Analyses of ocean color data acquired by the Coastal Zone Color Scanner (CZCS) on the research satellite Nimbus 7 [Gordon et al., 1980; Gordon and Morel, 1983; Hovis et al., 1980] have employed empirical algorithms to derive phyto-

plankton pigment concentration (the sum of the concentrations of chlorophyll *a* and its degradation product phaeophytin *a*) from atmospherically corrected radiances and semiempirical methods [Austin and Petzold, 1981] to derive the diffuse attenuation coefficient of the water in the blue-green region of the spectrum. Morel [1980] demonstrated the use of an analytic method to extract the pigment concentration from in-water diffuse reflectance measurements, even in waters where the presence of high turbidity can considerably alter their appearance. Such analytic procedures have yet to be extended to satellite observations because of the difficulty of achieving atmospheric correction of sufficient accuracy. Thus to increase the quality of the analysis of satellite observations of ocean color, better techniques of atmospheric correction are required. This was the original motivation for the work presented here.

As briefly described in the appendix, CZCS atmospheric correction is effected by assessing the radiance contribution of the atmosphere in spectral bands at which the radiance exiting the ocean is known and extrapolating the aerosol component of the atmospheric contribution to bands where the water-leaving radiance is desired in order to derive the pigment concentration. At present, this can be carried out directly only for picture elements (pixels) in the image where the pigment concentration is smaller than 0.25 mg m^{-3}, in which case the spectral water-leaving radiance $L_w(\lambda)$ is known at wavelengths, λ, of 520, 550, and 670 nm [Gordon and Clark, 1981]. For the rest of the image, where $L_w(520)$ and $L_w(550)$ are unknown, the aerosol is assumed to possess the same spectral behavior, an assumption which fails when the physical properties (size distribution and composition) of the aerosol are dependent on position. Thus it would be useful to be able to assess the aerosol properties at each individual pixel, or at least at a large enough number of pixels to be able to determine their low-frequency spatial variation. This of course requires knowledge of the scene water-leaving radiance in several spectral bands. In waters defined as Morel Case 1 [Morel and Prieur, 1977], i.e., waters for which phytoplankton and their associated debris control the optical properties, the water-leaving radiance should depend only on the pigment concentration. Therefore pixel-by-pixel atmospheric correction requires a relationship between spectral radiance and pigment concentration. In this paper, we model such a relationship.

The focus of our effort, unlike the models of Carder et al. [1985, 1986a, b], which were developed to explain data for a specific reflectance spectrum or data acquired in a given

---

[1]Department of Physics, University of Miami, Coral Gables, Florida.

[2]Rosentiel School of Marine and Atmospheric Sciences, University of Miami, Miami, Florida.

[3]University of California Marine Bio-Optics, CSL Center for Remote Sensing and Environmental Optics, University of California at Santa Barbara.

[4]University of California Marine Bio-Optics, Scripps Institution of Oceanography, University of California at San Diego, La Jolla.

[5]National Environmental Satellite Data Information Service, National Oceanic and Atmospheric Administration, Washington, D. C.

region, will be to model the totality of Case 1 waters, i.e., our model will be judged in a statistical sense by comparison with experimental data from a variety of Case 1 waters. We explain the "noisy" pigment-radiance relationship observed for pigment concentrations above about 0.25 mg m^{-3} [*Gordon and Clark*, 1981] in terms of the natural variation of the backscattering of the phytoplankton-detritus combination. Our model is similar to that presented by *Gordon and Morel* [1983], which shows that ratios of the diffuse reflectance at two wavelengths can be derived from the average optical properties of the suspended and dissolved material. Their derived ratios were found to be in excellent agreement with the statistically derived experimental counterparts. Here, however, we focus on the actual normalized water-leaving radiances, rather than just the ratios of diffuse reflectance. The basic optical model used here closely follows that of *Gordon and Morel* [1983].

In what follows, we first relate the normalized water-leaving radiance to the optical properties of the water and its constituents. Then an optical model of the dependence of the absorption and backscattering coefficients of the phytoplankton and their immediate detritus on the pigment concentration is described and is used to relate the radiance to the pigment concentration. The results are then compared with surface and satellite measurements. Finally, applications are described, and the model is extended to include the effects of other material often seen in the water, i.e., detached coccoliths from coccolithophorids.

THE RADIANCE MODEL

Preliminary Considerations

We start by defining the normalized water-leaving radiance [L_w]$_N$, following *Gordon and Clark* [1981],

$$[L_w]_N = \left[\frac{(1 - \rho)(1 - \bar{\rho})F_0 R}{m^2 Q(1 - rR)} \right] \quad (1)$$

where ρ is the Fresnel reflectance of the sea surface for normal incidence; $\bar{\rho}$ is the Fresnel reflection albedo of the sea surface for irradiance from the Sun and sky; F_0 is the mean extraterrestrial solar irradiance; R is the irradiance reflectance just beneath the sea surface ($R = E_u/E_d$, where E_u and E_d are the upwelling and downwelling irradiances just beneath the surface respectively; m is the index of refraction of water; and Q is the ratio of the upwelling radiance to the upwelling irradiance toward the zenith. Q equals π for a totally diffuse radiance distribution and, although it has received little experimental attention, appears to be between 4 and 5 and somewhat dependent on wavelength for radiance distributions observed in nature [*Austin*, 1979]. Note that the term $(1 - rR)$ in the denominator (where r, the water-air reflectance for totally diffuse irradiance, is about 0.48 and accounts for the effect of internal reflectance of the upwelling radiance field by the sea surface), which was left out of the definition of *Gordon and Clark* [1981], has been explicitly included in (1); however, it is relatively unimportant, since the maximum value of R in Case 1 waters is 0.08–0.10.

The value of ρ is found to be nearly independent of the wind speed [*Austin*, 1974] and can be taken to be 0.021 over the visible spectrum. The value of $\bar{\rho}$ depends in a complicated manner on the solar zenith angle θ_0 through the dependence of the relative amounts of direct sunlight and diffuse skylight incident on the sea surface. Here $\bar{\rho}$ is less than 0.1 when θ_0 is

less than 60°, which is the typical situation in most CZCS applications. *Plass et al.* [1975] and *Preisendorfer and Mobley* [1986] have shown that in the range $0 \leq \theta_0 \leq 60°$, $\bar{\rho}$ is practically independent of the wind speed. This means that it can be computed under the assumption that the ocean is flat. For $0 \leq \theta_0 \leq 60°$ the reflectivity of the direct solar beam is between 0.021 and 0.064, while the reflectance for totally diffuse skylight is 0.066. Therefore if a mean value of 0.043 is taken for $\bar{\rho}$, the factor $(1 - \bar{\rho})$ in (1) would be expected to vary between 0.934 and 0.979, or less than 3% about the mean of 0.957.

Normalized water-leaving radiance is that which would exit the sea surface if the Sun were at the zenith and if the atmosphere were absent, i.e., $L_w = [L_w]_N t(\theta_0) \cos \theta_0$, where t is the diffuse transmittance of the atmosphere [*Gordon et al.*, 1983b]. Thus it is meaningful to compare normalized water-leaving radiances for different locations and times. Equation (1) shows that [L_w]$_N$ is related to the optical properties of the water through R and Q in the combination R/Q. *Gordon* [1986] has recently carried out extensive computations of R/Q as a function of the optical properties of the water and the solar zenith angle θ_0 and has concluded that for $\theta_0 \geq 20°$, R/Q can be directly related to the inherent optical properties of the water [*Preisendorfer*, 1961, 1965], the absorption coefficient a, and the backscattering coefficient, b_b, through

$$\frac{R}{Q} = \sum_{i=1}^{2} l_i \left(\frac{b_b}{a + b_b} \right)^i \quad (2)$$

where $l_1 = 0.0949$ and $l_2 = 0.0794$. The error in (2) is significantly less than 10% for a wide range of realistic scattering phase functions. For $\theta_0 < 20°$, R/Q depends on the specific details of the scattering phase function in the backward direction. In order to use this relationship to compute [L_w]$_N$, one must relate a and b_b, spectrally, to the constituent concentrations in the water. For Case 1 waters, by hypothesis, only one constituent concentration is required: the phytoplankton pigment concentration C. There are two possibilities for accomplishing this. The direct method is to use the absorption coefficient of water a_w and the specific absorption coefficient a_c^* of phytoplankton [*Morel and Prieur*, 1977], i.e., $a = a_w + a_c^* C$, or one of the more recent models of phytoplankton absorption given by *Prieur and Sathyendranath* [1981], and then to develop a relationship between b_b and C [*Gordon and Morel*, 1983; *Morel*, 1980]. The indirect method is to circumvent the use of a by noting that K, the downwelling irradiance attenuation coefficient, can be related to $a + b_b$. *Gordon et al.* [1975] show that

$$\frac{K}{cD_0} = \sum_{i=0}^{3} k_i \left(\frac{b_f}{c} \right)^i \quad (3)$$

where c is the beam attenuation coefficient ($c = a + b$, where b is the scattering coefficient), b_f is the forward scattering coefficient ($b = b_f + b_b$), $k_0 = 1.000$, $k_1 = -0.996$, $k_2 = 0.109$, and $k_3 = -0.153$. On the basis of more recent computations [*Gordon*, 1986], a more satisfactory relationship can be derived, i.e.,

$$\frac{K}{cD_0} = \sum_{i=1}^{2} \kappa_i \left(1 - \frac{b_f}{c} \right)^i \quad (3')$$

with $\kappa_1 = 1.054$ and $\kappa_2 = -0.021$. Also, in the limit of large b_f/c a very good fit to the computations is obtained with $\kappa_1 = 1.083$ and $\kappa_2 = 0$. In (3) and (3'), D_0 is the downwelling

distribution function [*Preisendorfer*, 1961] evaluated for $c = a$ (i.e., no scattering) and effectively provides the dependence of K on the geometrical structure of the in-water light field. D_0 depends on the radiance distribution incident on the sea surface. It can be determined from a knowledge of the relative amounts of direct sunlight and diffuse skylight at the sea surface [*Gordon*, 1976]. For a clear atmosphere the relative amounts of sunlight and skylight depend on the wavelength, with the skylight component increasing with decreasing wavelength at the expense of the direct sunlight component. For the direct sunlight component, $D_0 = 1/\cos \theta_{0w}$, where θ_{0w} is the solar zenith angle measured beneath the sea surface. In the case of the range of Sun angles applicable to the data which follows, this component falls in the range $1 \leq D_0 \leq 1.18$. The skylight component has $D_0 \cong 1.2$, under the assumption that it is totally diffuse; otherwise, it is also between 1 and 1.2. Thus for all of the data which we shall be examining, D_0 will always be in the range 1.0–1.2. D_0 is nominally set to 1.1 in the computations presented here, and the resulting error in $[L_w]_N$ due to this quantity should be less than $\pm 10\%$. Note that by definition, $K = aD_0$ when there is no scattering, i.e., $c = a$. Equation (3) clearly satisfies this limit, but (3') does not. However, the error in K is only about 2% at this limit, which is compatible with the average error in K over the full range of b_f/c.

If the terms for $i > 1$ are ignored in (2) and (3'), we find

$$R/Q = l_1 \frac{b_b}{a + b_b} \qquad (4)$$

and

$$K = \kappa_1 c D_0 \left(1 - \frac{b_f}{c}\right) = \kappa_1 D_0 (a + b_b) \qquad (5)$$

so that $R/Q = l_1 \kappa_1 D_0 b_b / K$. By definition, l_1, κ_1, and D_0 are independent of the pigment concentration, so, finally,

$$R/Q = 0.110 \frac{b_b}{K} \qquad (6)$$

The accuracy of (6) is limited by the error caused by ignoring the terms with $i > 1$ in (2) and (3'). Since $l_2 \approx l_1$, the fractional error in R/Q caused by dropping the $i = 2$ term in (2) is approximately $X/(1 + X)$, where $X = b_b/(a + b_b)$. The largest value of X used in this study is ≈ 0.2, so the maximum error in (4) is $\approx 16\%$. Since $\kappa_2 \approx \kappa_1/50$ and the maximum $(1 - b_f/c)$ is 1, the maximum error resulting from dropping κ_2 in (3') is 2%. Typically, the error is about 1%. Thus the maximum rms error in (6) from all sources is less than $\approx 20\%$.

Since it is only of second order in importance, the remaining term, $1/(1 - rR)$, in (1) can be computed with sufficient accuracy from R/Q, using the approximation $Q = \pi$, i.e., by multiplying R/Q from (6) by π. Hence using (1), $[L_w]_N$ variations can be explained in terms of variations in K and b_b, and these quantities must then be related to C. It should be noted that unlike earlier models [*Carder et al.*, 1985, 1986a, b; *Gordon and Morel*, 1983] which actually modeled the diffuse reflectance, R, this is a direct model of the water-leaving radiance itself.

Choice of Model Parameters

Although, K is not an inherent optical property and therefore does not rigorously satisfy Beer's law (in contrast to a), *Smith and Baker* [1978a, b] and *Baker and Smith* [1982] had

considerable success in modeling the results of experimental measurements in Case 1 waters (and those waters where absorption, rather than scattering, is the dominant contribution from each of the attenuating constituents) with

$$K = K_w + K_c + K_{ys} \qquad (7)$$

where K_w, K_c, and K_{ys} are the partial contributions to K due to water, phytoplankton, and optically relevant dissolved organic material, called yellow substances (YS). K_c is the value of $K - K_w$ for a given C in waters for which YS were believed to play a minor role in the determination of K. It was approximated as a function of C by the envelope of the minimum values of K. *Baker and Smith* [1982] determined that

$$K_c = k_c C \exp \left\{ -[k_c' \log_{10} (C/C_0)]^2 \right\} + 0.001C^2 \qquad (8)$$

where k_c, k_c', and C_0 are dependent on wavelength and are tabulated for $C < 10$ mg m^{-3}. Note that in (8), K depends on C in a nonlinear manner. This is a manifestation of the fact [*Hobson et al.*, 1973; *Smith and Baker*, 1978a] that as the concentration of phytoplankton increases (and thus the pigment concentration also), the ratio of phytoplankton carbon to detrital carbon also increases. Thus in the two-component absorption system of phytoplankton and its detrital material, the relative amounts of the components vary with the pigment concentration, forcing the total absorption to be a nonlinear function of the pigment concentration. In addition, as the chlorophyll concentration, and hence the pigment biomass and scattering, increases, the attenuation due to phytoplankton is increasingly influenced by scattering. This scattering contribution to the diffuse attenuation due to phytoplankton is nonlinear, and the departure from Beer's law is accommodated empirically in the Baker and Smith bio-optical model.

The absorption of YS is known to increase approximately exponentially with decreasing wavelength from the visible to the ultraviolet, i.e.,

$$a_{ys}(\lambda) = a_{ys}(\lambda_r) \exp \left[-S(\lambda - \lambda_r) \right] \qquad (9)$$

where λ_r is a reference wavelength usually in the ultraviolet. S determines the spectral dependence a_{ys} and is found to be approximately 0.014 nm^{-1} [*Bricaud et al.*, 1983b, and references therein]. The concentration of YS is specified by providing $a_{ys}(\lambda_r)$. The measurements of *Bricaud et al.* [1983b] for oceanic waters indicate that in some oceanic areas, e.g., the equatorial divergence in the Gulf of Guinea, or areas not influenced by fresh water, e.g., the Mauritanian upwelling region, there appears to exist a minimum or "background" YS concentration which is independent of C but which vanishes for oligotrophic waters such as the Sargasso Sea. This background concentration corresponds to $a_{ys}(375) = 0.06$ m^{-1}. Above this background, there is a fluctuating component which is also independent of C.

Since YS are dissolved and for all practical purposes do not scatter, (5) shows that $K_{ys} \approx D_0 a_{ys}$. Therefore K_{ys} can be assumed to be proportional to a_{ys}. In the Baker-Smith determination of K_c, the fluctuating component appears as noise above the $K - C$ envelope and thus would not be included in their K_c. In contrast, the background would provide a constant addition to K for all C, except in the oligotrophic waters, and hence would be included in the envelope estimating K_c. Note, however, that the experimental data used by Baker and Smith for the lowest pigment concentration were measured in the Sargasso Sea, which is virtually free of YS, so their K_c at very low pigment concentration is free from the YS back-

ground. Therefore we conclude that the optical effect of any background component of the YS is already included in K_c. K_c also includes the optical effect of any natural phytoplankton detritus, e.g., fragments of broken cells, etc., which may covary with C. We take

$$K_{ys}(\lambda) = D_0[a_{ys}(375) - 0.06] \exp[-0.014(\lambda - 375)] \quad (10)$$

and use (10) only for the fluctuating YS component. Equations (7), (8), and (10) are adopted for the estimation of K in (6).

It remains only to relate b_b to the phytoplankton pigment concentration. We note first that b_b contains a component due to phytoplankton and their associated detrital material, $(b_b)_p$, and a component due to pure seawater, $(b_b)_w$, i.e.,

$$b_b = (b_b)_w + (b_b)_p$$

Then we define the backscattering probability $\tilde{b}_b$,

$$b_b = \tilde{b}_b b$$

and note that for Case 1 waters the scattering coefficient at 550 nm has been empirically related to the pigment concentration [Morel, 1980] through

$$b(550) = b^0 C^{0.62} \quad (11)$$

where, if C is numerically equal to the pigment concentration in milligrams per cubic meter, b^0 ranges from 0.12 to 0.45 m^{-1}, with a mean value of 0.3 m^{-1} adopted by Gordon and Morel [1983]. Since the total scattering due to pure seawater is significantly less than the total scattering by particulates (mostly in the forward direction), we can take $b(550)$ to represent the particulate scattering alone. The wide variation in scattering for a given C implied by (11) (about a factor of 4) is, at least in part, due to variations in the species composition of the waters under examination. Bricaud et al. [1983a] have shown that the specific scattering coefficient (scattering per unit pigment concentration) varied by nearly an order of magnitude over the four species which were studied. Another source of this natural scattering variability is variation in the relative concentrations of phytoplankton and phytoplankton detrital particles. It is interesting to note that although the relationship between K and C is also empirical, the data for Case 1 waters do not show the large variance about the mean curve that the scattering data show (compare Gordon and Morel [1983, Figures 5 and 7]). Measurements of oceanic and coastal volume-scattering functions indicate that b_b is usually only 1–2% of b, which implies that for most Case 1 waters at moderate pigment concentrations, $a \gg b_b$. Thus K is largely determined by the absorption coefficient, and hence its variation with C is determined by the variation of the absorption of phytoplankton and their associated detrital material with C. Sathyendranath [1981], in examination of the specific spectral absorption coefficient $a_c{}^*(\lambda)$ for five species of cultured phytoplankton, finds that when normalized to one wavelength (440 nm), they all have essentially the same spectrum. Furthermore, this spectrum agrees very well with that determined for naturally occurring phytoplankton (normalized in the same manner) by Prieur and Sathyendranath [1981]. Thus the phytoplankton absorption can be reasonably well characterized by a species-dependent specific absorption coefficient at a single wavelength and a species-independent normalized spectrum. The specific absorption coefficient shows only about a threefold variation over the same species for which Bricaud et al. [1983a] found a tenfold variation in the specific scattering coefficient. This is believed to be one of the reasons for the

less erratic $K - C$ relationship in comparison with the $b - C$ relationship. Variation in the relative amount of phytoplankton and detrital absorption for a given pigment concentration apparently is not sufficiently large to produce strong scatter in the $K - C$ relationship.

As mentioned earlier, the backscattering probability for seawater is generally about 1–2%, and indeed, Gordon and Morel [1983] found that assuming $(\tilde{b}_b)_p = 0.01$ yielded excellent agreement between observed and computed values of $R(440)/R(560)$ for pigment concentrations up to 3–5 mg m^{-3}. However, they also found that the agreement could be extended to higher pigment concentrations by accounting for the variation of the backscattering coefficient with the pigment concentration and with the wavelength. We can understand the effect of pigment concentration on the particle backscattering coefficient in Case 1 waters by noting that phytoplankton have been determined to exhibit very low backscattering, i.e., $(\tilde{b}_b)_p \sim 0.5\%$ [Morel and Bricaud, 1981]. At low pigment concentration most of the particle backscattering results from scattering by phytoplankton detrital material e.g., fragments of broken cells, etc. As the phytoplankton concentration increases, the ratio of viable phytoplankton to detrital particles also increases, so at higher concentrations the phytoplankton have a relatively larger effect on the optical properties of the medium than they do at lower concentrations (see the earlier discussion concerning the nonlinear relationship between K_c and C). Thus we expect the particle backscattering probability $(\tilde{b}_b)_p$ to decrease as the pigment concentration increases, and we assume that at 560 nm, $(\tilde{b}_b)_p$ varies from 2% at $C = 0.1$ mg m^{-3} to 0.5% at $C = 20$ mg m^{-3}.

Following Gordon and Morel [1983], we assume that $(b_b)_p$ varies with wavelength and pigment concentration according to the law

$$(b_b)_p = A(\lambda)C^{B(\lambda)} \quad (12)$$

where $A(\lambda)$ and $B(\lambda)$ are wavelength-dependent constants, with $A(\lambda) \propto b^0$. The influence of wavelength on $(b_b)_p$ is established on the basis of two observations: (1) at low pigment concentrations $(C < 0.1$ mg m$^{-3})$ the scattering coefficient b for ocean water exhibits approximately a λ^{-1} wavelength dependence; and (2) at wavelengths at which particles are strongly absorbing, their scattering is reduced such that their total attenuation is only weakly dependent on wavelength. Thus if for the purposes of the present model all the wavelength dependence of $(b_b)_p$ is placed into $(\tilde{b}_b)_p$, $(\tilde{b}_b)_p$ for $C < 0.1$ mg m^{-3} should be $(560/\lambda) \times 2\%$, and to account for the depressive effects of absorption on scattering, $(\tilde{b}_b)_p$ is taken to be 0.3% for $C = 20$ mg m^{-3} at wavelengths within the pigment absorption bands and 0.5% outside the bands. These limits combined with (11) establish the constants $A(\lambda)$ and $B(\lambda)$ in (12). The resulting values of these constants for the wavelengths used in the work with $b^0 = 0.3$ m^{-1} are given in Table 1, along with the backscattering of pure seawater derived from the measurements of Morel [1974]. This defines all of the parameters required in (6) to relate $[L_w]_N$ to C, using (1).

COMPARISON WITH EXPERIMENTAL DATA

Surface Data

We now compare the results of this model with the experimental data for Case 1 waters collected by Clark [1981] in support of the effort to establish pigment algorithms for the

TABLE 1. Parameters A and B Used in the Model, Along With $(b_b)_w$

λ, nm	A ($\times$ 1000), m^{-1}	B	$(b_b)_w$ ($\times$ 1000), m^{-1}
443	3.0	0.22	2.47
520	3.3	0.35	1.20
550	3.3	0.36	0.97

CZCS. Figures 1, 2, and 3 provide the normalized radiance at 443, 520, and 550 nm, respectively, as a function of the pigment concentration derived from Clark's data (points), along with the computations from the model described previously (lines). The vertical bars on the data points are used to indicate an estimated $\pm 10\%$ error in the experimental radiance measurement. The three curves correspond to different values of the scattering coefficient at 550 nm for a pigment concentration of 1 mg m^{-3}, i.e., b^0. The lower curve corresponds to $b^0 = 0.12$ m^{-1}, which gives the lowest scattering coefficient observed for a given pigment concentration in waters believed to satisfy the criteria for being classified as Case 1. Similarly, the upper curve is for $b^0 = 0.45$ m^{-1}, which gives the largest scattering observed in Case 1 waters. Finally, the middle curve results from the mean value of b^0, chosen by *Gordon and Morel* [1983] to be 0.30 m^{-1}. The concentration of YS over and above the "background" is taken to be zero, i.e., the "background" YS concentration, as described earlier, has been assumed to be included in K_c, and $a_{ys}(375)$ in (10) is taken to be 0.06 m^{-1}. Nearly all of the data are seen to fall between the limiting curves characteristic of the observed natural variability in scattering for Case 1 waters. In fact, considering the estimated 10% error associated with the experimental measurements, all of the data, with one exception, fall within this limiting range. This is particularly significant, because the data used to specify the model parameters were obtained in different regions of the world's oceans. The scattering data of Morel and coworkers relating b and C were mostly collected off the African coast and in the Meditteranean Sea, with a few samples from the Sargasso Sea. The irradiance data of Smith
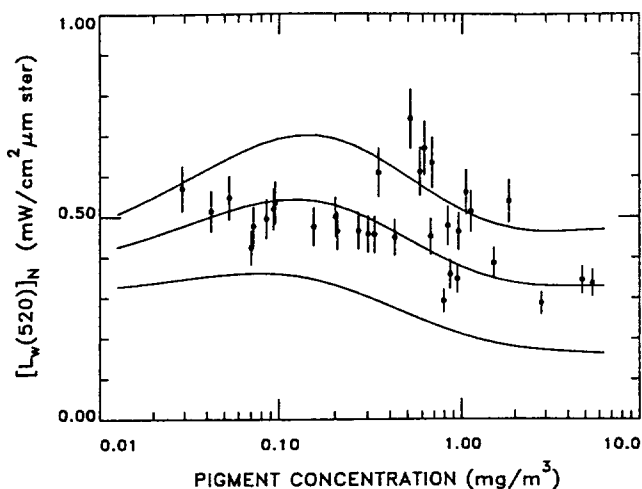

Fig. 2. Value of $[L_w(520)]_N$ as a function of the pigment concentration. The curves are the results of the model, with the upper curve corresponding to $b^0 = 0.45$ m^{-1}, the middle curve to $b^0 = 0.30$ m^{-1}, and the lower curve to $b^0 = 0.12$ m^{-1}. The points are Clark's [1981] experimental measurements.

and Baker, providing the relationship between K and C, were for the most part collected in the Pacific off the California coast, with a few samples from the Sargasso Sea. Clark's radiance-C data were collected in the Middle Atlantic Bight, the Gulf of Mexico, the Sargasso Sea, and the Gulf of California. The close agreement between the model and the measurements is remarkable, and it attests to the care exercised by the investigators in calibration and in performing the measurements. It also suggests that waters which by definition belong to Case 1 seem to have similar optical properties, within well-defined limits, regardless of their location (however, see later discussion) and that an algorithm for retrieving C from $[L_w(\lambda)]_N$ which is developed in a particular subset of Case 1 waters, i.e., in a particular region, may have far wider applicability.

It is also gratifying that the envelope of the minimum radiance for a given C appears to follow closely the predictions of
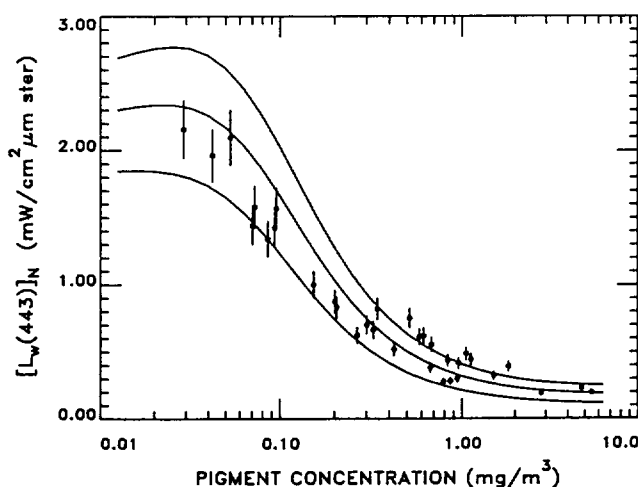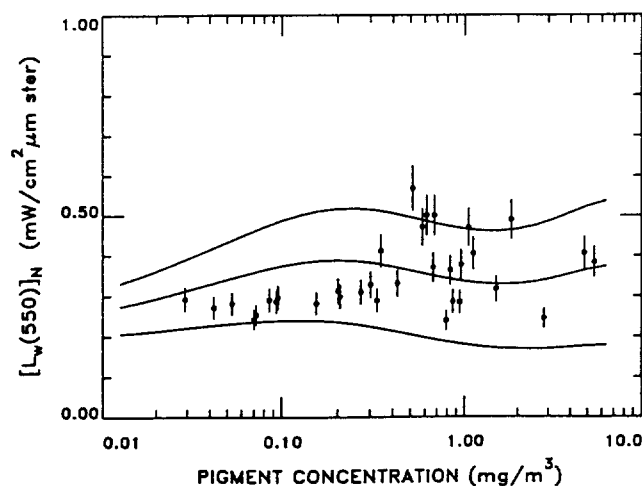

Fig. 1. Value of $[L_w(443)]_N$ as a function of the pigment concentration. The curves are the results of the model with the upper curve corresponding to $b^0 = 0.45$ m^{-1}, the middle curve to $b^0 = 0.30$ m^{-1}, and the lower curve to $b^0 = 0.12$ m^{-1}. The points are Clark's [1981] experimental measurements.

Fig. 3. Value of $[L_w(550)]_N$ as a function of the pigment concentration. The curves are the results of the model, with the upper curve corresponding to $b^0 = 0.45$ m^{-1}, the middle curve to $b^0 = 0.30$ m^{-1}, and the lower curve to $b^0 = 0.12$ m^{-1}. The points are Clark's [1981] experimental measurements.
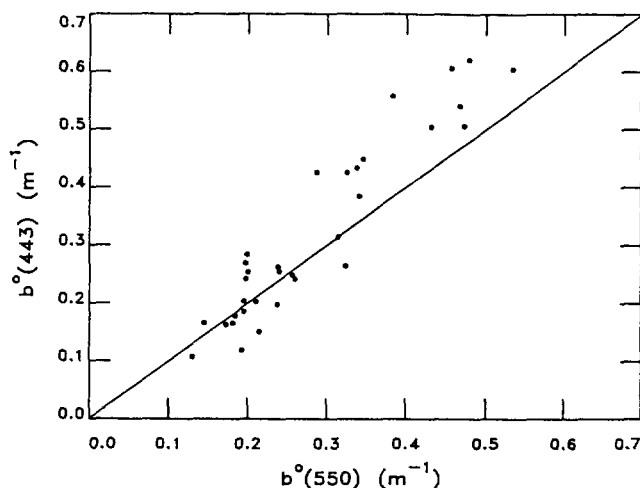
Fig. 4. Values of b^0(443) and b^0(550) required to bring the model predictions and Clark's [1981] experimental measurements into agreement.

the model. This suggests that the model can be used to determine the minimum water-leaving radiance to be expected for a given pigment concentration, a fact which will be very useful in application to image analysis.

The model clearly attributes the large scatter in the data for $C \geq 0.4$ mg m^{-3} to variations in the backscattering coefficient of the phytoplankton which make it difficult to estimate the pigment concentration from the radiance in a single band, even in the blue. However, given the pigment concentration, it appears that the model may be capable of broadly classifying the scattering characteristics of the phytoplankton. This suggests a possible avenue for deriving some species-dependent information from ocean color observations.

Examination of Figures 1-3 indicates that it is not possible to find a single value of b^0 which will fit the experimental data at all wavelengths. However, this is to be expected because each individual station is likely to be characterized by a different value of b^0, so the key question is, will a single value of b^0 suffice to characterize $[L_w(\lambda)]_N$ for a given location? To answer this question, we have inverted the model to compute the values of $b^0(\lambda)$, which will bring the model and the observations into agreement for each measurement. The results are provided in Figure 4, in which b^0(443) and b^0(550) are compared, and Figure 5, in which b^0(520) and b^0(550) are compared. (Note that the notation $b^0(\lambda)$ does not mean the value of b^0 at the wavelength λ, but rather, it stands for the value of b^0 at 550 nm that will produce agreement between the observed and measured $[L_w]_N$ at the wavelength λ). Figures 4 and 5 show that the required b^0 are approximately linearly related to one another, but there appears to be an offset bias between the various wavelengths, e.g., for a given station the required b^0 at 520 nm is somewhat higher than that at 550 nm. In fact, comparison of Figures 2 and 3 (or Figure 5) shows that at low pigment concentration $(C \leq 0.4$ mg m$^{-3})$ a value of 0.26 m^{-1} is desirable at 520 nm, while a value of about 0.20 m^{-1} is required at 550 nm to bring the model into agreement with the data. This particular bias may result from a small systematic error in the calibration of the radiometric data.

This model can of course also be used to compute radiance ratios as a function of the pigment concentration. As mentioned earlier, Figures 1 and 3 show that a value of $b^0 \approx 0.2$ m^{-1} fits the experimental radiance very well in the low range

of the pigment concentration. Figure 6 compares the ratio of the normalized radiances at 443 and 550 nm computed using the model with $b^0 = 0.2$ m^{-1} with Clark's experimental data. It is noteworthy that the variance in the radiance data, compared to the model for $C > 0.4$ mg m^{-3}, is considerably reduced in the ratio. Figure 7 similarly shows the ratio of the normalized radiances in the two green bands as a function of C. Again, the scatter is considerably reduced, but in this case the model does not predict the correct ratio because the data at these two bands favor considerably different values of b^0. Choosing different values of b^0 for each wavelength improves the fit; however, no combination of values appears to provide as satisfactory a fit as that in Figure 6. The reduction in the scatter realized in the ratios as compared to the individual radiances is significant. It shows that the radiance ratios are somewhat immune to the natural variation in phytoplankton backscattering, which is likely to be one of the reasons for the success of ratio algorithms [Clark, 1981; Gordon and Clark, 1980; Gordon et al., 1983b; Morel, 1980; Smith and Baker, 1982; Smith and Wilson, 1981] in the retrieval of pigment concentrations. But more importantly, it suggests that a universal ratio algorithm can be used to estimate C in Case 1 waters independently of the scattering variation. This could provide the estimate of C needed to derive the species-related information mentioned earlier.

Comparison of Figures 6 and 7 shows that the ratio $[L_w(443)]_N/[L_w(550)]_N$ is more sensitive to changes in the pigment concentration than the ratio $[L_w(520)]_N/[L_w(550)]_N$, provided that $C \leq 5$ mg m^{-3}, suggesting that the blue-green ratio should be used for estimating the pigment concentration up to this level. Furthermore, the model provides a far better fit to the data in Figure 6 than the linear fits [log $C = \log \alpha + \beta \log$ (ratio)] presently in use. We recommend using the model with $b^0 = 0.2$ m^{-1}, which provides the best fit to the data in Figure 6 over the entire range of pigment concentrations. (Note that the ratios presented in Figures 6 and 7 are ratios of normalized water-leaving radiances and will differ somewhat from ratios of unnormalized radiances.) At the higher pigment concentrations most of the variation in the blue-green ratio is due to $[L_w(443)]_N$, and this variation is very small, i.e., about 0.1 mW cm^{-2} μm sr, as C varies from 1 to 5 mg m^{-3}. Under
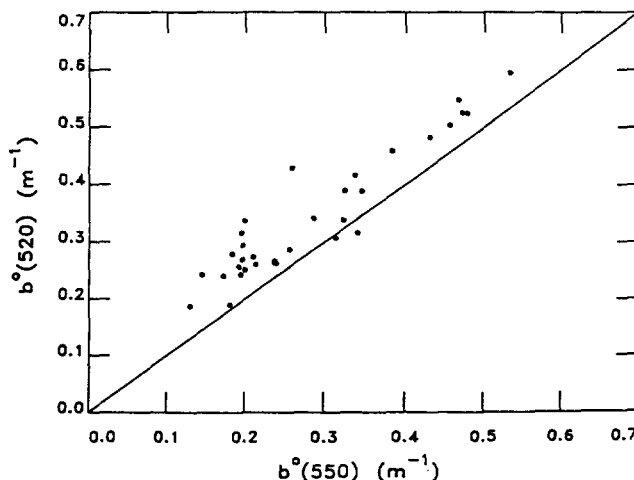

Fig. 5. Values of b^0(520) and b^0(550) required to bring the model predictions and Clark's [1981] experimental measurements into agreement.

optimum viewing conditions, i.e., small θ_0 and a clear atmosphere, this represents a variation in L_w of a little over two CZCS digital counts (DC); however, because the radiometric sensitivity of the CZCS degraded with time in orbit [*Gordon et al.*, 1983a], the actual variation in L_w over this pigment range could be less than 1 DC. (At launch, 1 DC $\cong$ 0.045, 0.031, and 0.025 mW cm^{-2} μm sr, at 443, 520, and 550 nm, respectively). Thus the sensitivity of this ratio at high pigment concentrations ($\sim$1–5 mg m^{-3}) is poor in the CZCS; however, designs for future sensors such as the Ocean Color Imager [*Walsh*, 1982] have expanded radiometric sensitivity, which will partially overcome this problem.

As mentioned earlier, the model suggests the possibility of obtaining additional information concerning the bio-optical state of the water, over and above the pigment concentration. The extra information is, of course, an estimate of b^0. The methodology for this is straightforward: first, use Figure 6 to determine the pigment concentration (recall that this ratio is nearly independent of b^0; then, given C, the model is inverted using $[L_w(550)]_N$ to estimate b^0. This band is ideal for the b^0 estimation, since the model indicates that $[L_w(550)]_N$ is only weakly dependent on the pigment concentration, and hence errors in the estimate of C will only weakly influence the resulting b^0. The data in Figure 3 show a total variation in $[L_w(550)]_N$ of about 0.32 mW cm^{-2} μm sr or about 13 CZCS DCs. If atmospheric correction can be performed to an accuracy of about 1–2 DC at 550 nm, then it is possible to broadly classify the scattering parameter b^0 into three levels: $b^0 < 0.25$ m^{-1}; $0.25 < b^0 < 0.35$ m^{-1}; and $b^0 > 0.35$ m^{-1}, i.e., "soft," "medium," and "hard" scatterers. For a relatively clear atmosphere ($L_a(670) \sim 0.5$ mW cm^{-2} μm sr) this requires the atmospheric correction parameter $\varepsilon(550, 670)$ (see the appendix) to be known to slightly better than ±0.1, while for more turbid atmospheres a correspondingly more accurate value of ε is required. Typically, $0.9 \leq \varepsilon(550, 670) \leq 1.2$, so choosing a mean of 1.05 implies a maximum error $\delta\varepsilon = \pm0.15$, which is very near the required accuracy for a relatively clear atmosphere. The key then to using a technique such as this to find both C and b^0 in the general case is an accurate determination of the atmospheric correction parameters ε.
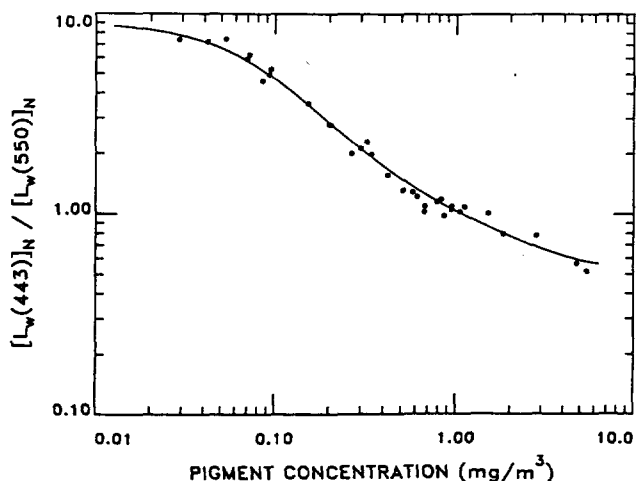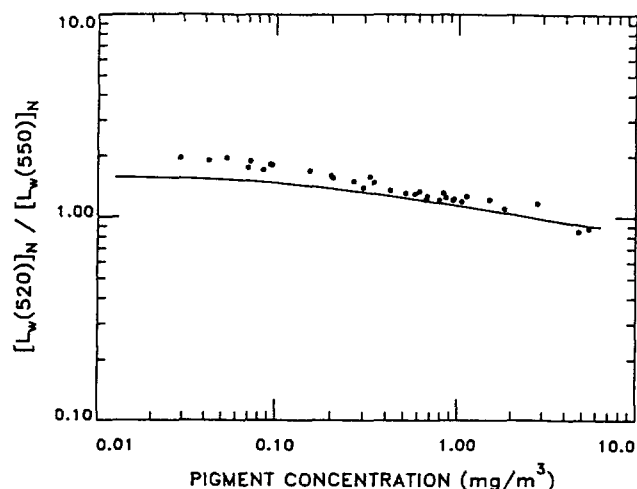

Fig. 7. The radiance ratio $[L_w(520)]_N/[L_w(550)]_N$ as a function of the pigment concentration. The curve is the result of the model, with $b^0 = 0.20$ m^{-1}. The points are *Clark's* [1981] experimental measurements.

Satellite Data

For the waters which may be classified as Case 1, the model predicts that in the absence of variations in the scattering properties of the phytoplankton and their associated detrital material, as manifested by variations in b^0, the normalized water-leaving radiance $[L_w(\lambda)]_N$ at 520 and in particular at 550 nm should depend very little on the pigment concentration. That is, in Figures 2 and 3 the model shows that for a given value of b^0 the variation of $[L_w(\lambda)]_N$ around their low-C values should be less than about $\pm20\%$. The radiance at 443 nm, on the other hand, is very strongly dependent on the pigment concentration in the range $0.1 \leq C \leq 1.0$ mg m^{-3}. Thus aside from the scattering variations, any variations in pigment concentration in this range should lead to strong variations in the radiance in the blue combined with little radiance variation in the green. At still higher pigment concentrations the ocean would essentially become a blackbody in the blue, again, with little or no variation in the green. An example of these observations is presented in Plate 1, which provides CZCS imagery of $[L_w(\lambda)]_N$ and C of the Middle Atlantic Bight, Georges Bank, and the Gulf of Maine from orbit 3240 (June 15, 1979). This image was atmospherically corrected, using values of the atmospheric correction parameters ε determined in the warm core ring near the center of the image. The standard bio-optical algorithms produced excellent agreement between ship-measured and satellite-estimated pigment concentrations along a ship track from Georges Bank north of the ring to the western edge of the image [*Gordon et al.*, 1983b]. Figure 8 provides the values of $[L_w(\lambda)]_N$ at 443, 520, and 550 nm along the line from the warm core ring across Georges Bank into the Gulf. The data are extracted from 100 equally spaced points (indicated by "entry number" on Figure 8) along the track and have been smoothed by applying a five-point running average. Along the line the pigment concentration varies from about 0.07 mg m^{-3} in the ring to near 1 mg m^{-3} on Georges Bank to about 0.3–0.5 mg m^{-3} in the Gulf of Maine. The variation in the $[L_w(\lambda)]_N$ is similar to that predicted by the model, i.e., a very large variation in $[L_w(\lambda)]_N$ in the blue accompanied by relatively small variations in $[L_w(\lambda)]_N$ at 520 and 550 nm. The variance in $[L_w(520)]_N$ and $[L_w(550)]_N$ is seen to fall within the confines of *Clark's* [1981]

Fig. 6. The radiance ratio $[L_w(443)]_N/[L_w(550)]_N$ as a function of the pigment concentration. The curve is the result of the model, with $b^0 = 0.20$ m^{-1}. The points are *Clark's* [1981] experimental measurements.
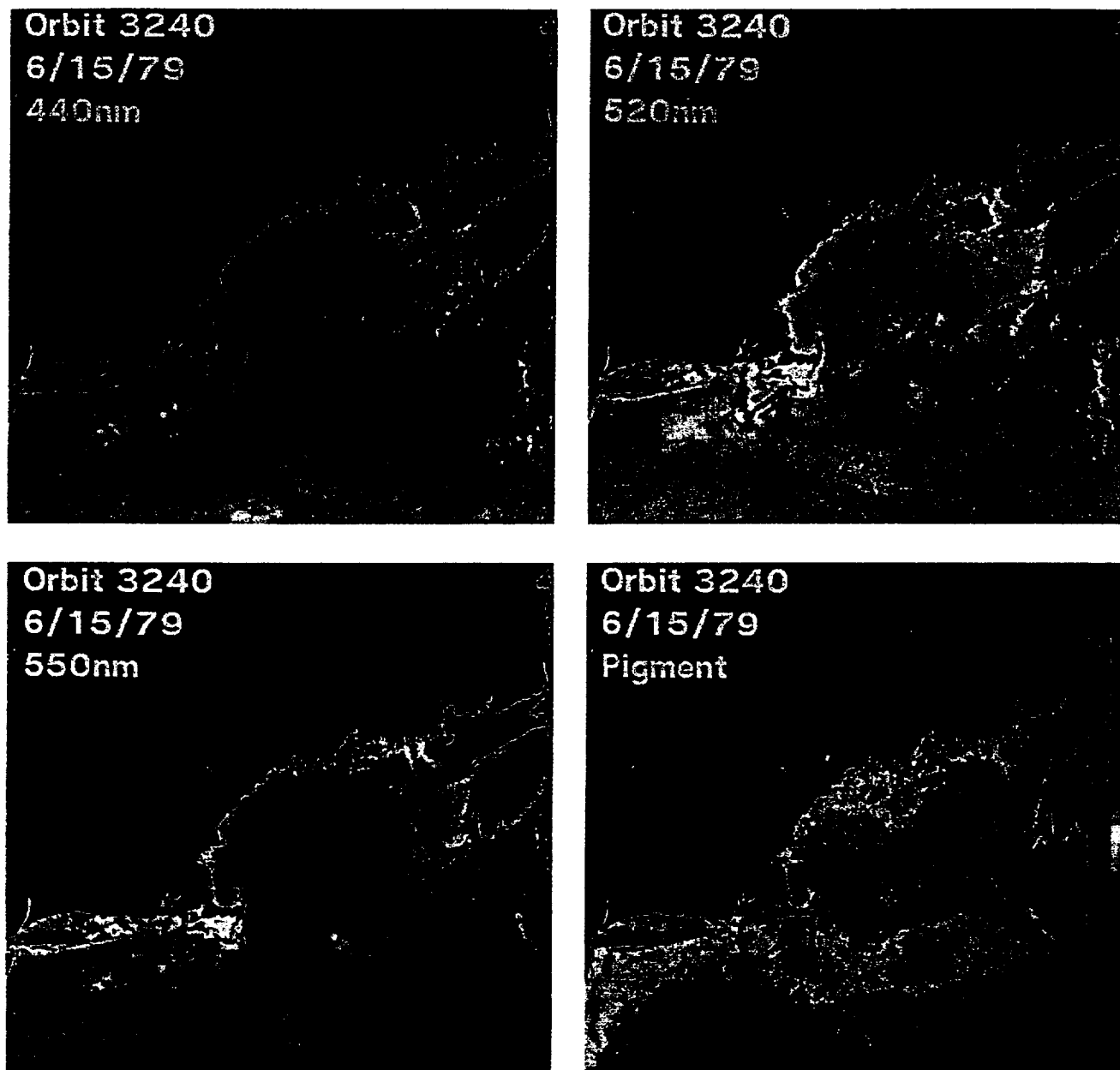
Plate 1. Image of $[L_w(443)]_N$, $[L_w(520)]_N$, $[L_w(550)]_N$, and C from orbit 3240 (June 15, 1979), with a track placed on the image.
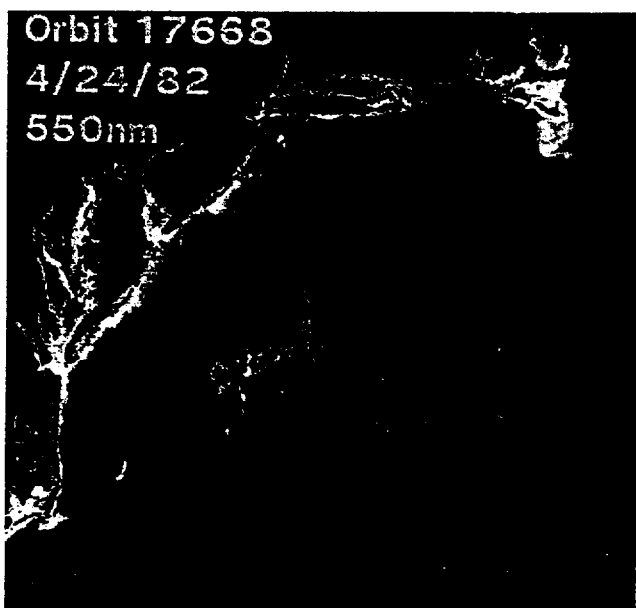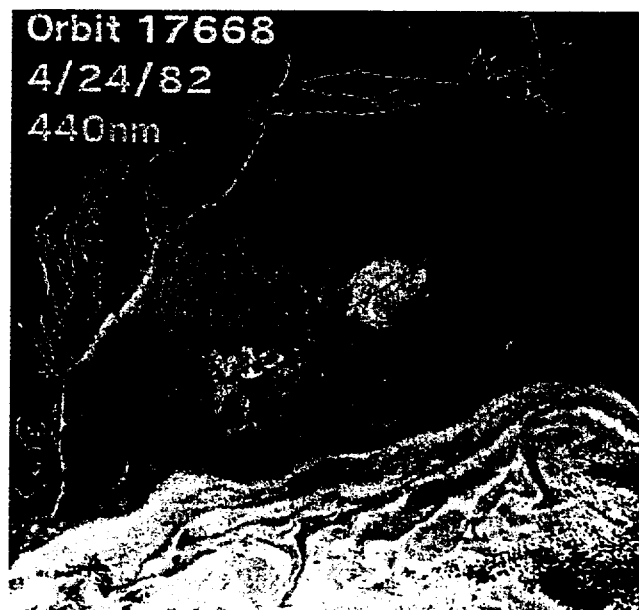
Plate 2. Image of $[L_w(443)]_N$, $[L_w(520)]_N$, $[L_w(550)]_N$, and C from orbit 17,668 (April 24, 1982), with two tracks placed on the image.
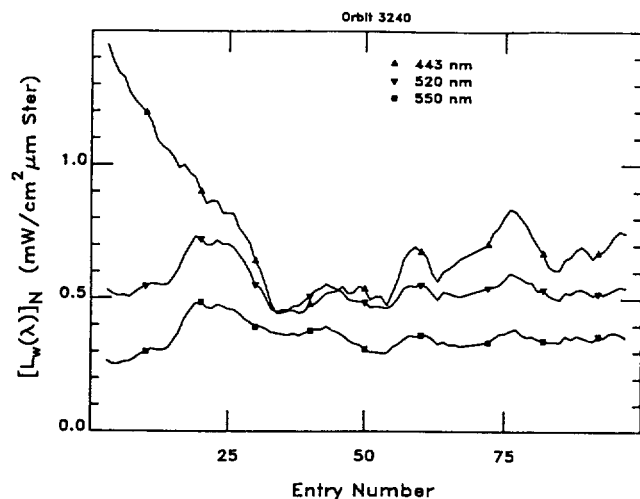
Fig. 8. Extracted values of $[L_w(443)]_N$, $[L_w(520)]_N$, and $[L_w(550)]_N$ along the track in Plate 1.
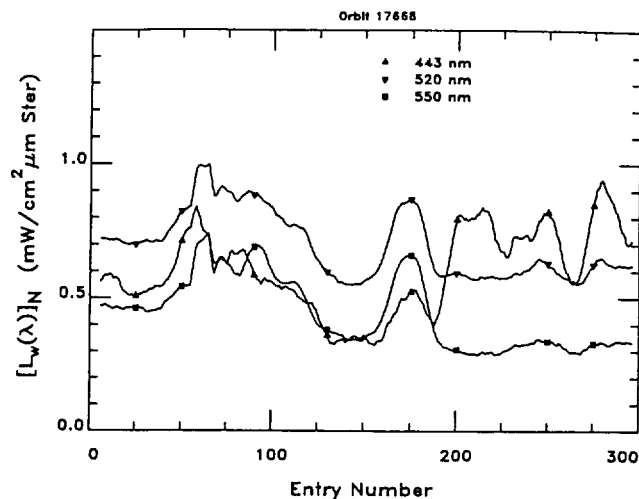

Fig. 9. Extracted values of $[L_w(443)]_N$, $[L_w(520)]_N$, and $[L_w(550)]_N$ along the red track in Plate 2.

experimental data and thus can be explained by Case 1 variations in b^0. Also, the variations of $[L_w(\lambda)]_N$ at 520 and 550 nm are highly correlated, supporting the contention that most of the variation in these bands is due to variations in scattering. This image is an example for which the model provides an adequate explanation of the observed radiance variations.

There are situations for which the model fails to explain the radiance variations, e.g., regions that show significant and simultaneous radiance variations in all three spectral bands over and above those expected on the basis of the natural variations in b^0 observed in Case 1 waters. Plate 2 shows an example of $[L_w(\lambda)]_N$, along with the pigment concentration computed from an image of the Middle Atlantic Bight acquired on April 24, 1982, in conjunction with the Warm Core Rings Experiment. In contrast to the image in Plate 1, in which the slope waters show low productivity, this image was acquired during the spring bloom when the pigment concentrations reached ≈ 5 mg m^{-3} [Brown et al., 1985]. This image was atmospherically corrected using ε determined in the clear-water regions of the Gulf Stream. The blue image taken alone would suggest that there are three regions of low pigments: the Gulf Stream, the Warm Core Ring (WCR) near the center of the image, and the bright area southwest of the ring. Examination of the two green bands shows the characteristically low variation in the radiance (especially at 550 nm) over most of the image, except for the very bright area to the southwest of the ring which was seen in the blue image as well. Thus on the basis of the radiance model, there is no justification for assuming that this particular area is low in pigments. It is interesting to note that a second WCR to the southwest of this bright area is clearly visible in the green imagery, while only a trace of it can be seen in the blue. This second WCR must have a high pigment concentration by virtue of its low radiance in the blue, but the appearance of structure in the green bands indicates that there must be significant variations in scattering. In fact, we believe, as the model suggests, that virtually all of the structure that is seen in the two green bands in this image, and especially that seen at 520 and 550 nm, is due to variations in scattering. It is useful to quantify the variations in radiance over some of the features of the image in Plate 2. For this purpose we have extracted the normalized water-leaving radiances along the red and

green tracks drawn on the image. In this case the data were extracted at 300 points along each track, and a 10-point running average was computed. The result of this extraction is shown in Figures 9 and 10 for the red and green tracks, respectively. Maximum radiances of 1.0, 1.3, and 1.1 mW cm^{-2} μm sr for 443, 520, and 550 nm, respectively, were observed near entry number 60 (close to where the two tracks intersect). These maxima do not appear on the graphs because of the considerable smoothing caused by the averaging procedure. Over both tracks, with the exception of the low pigment regions, i.e., the Gulf Stream (entry numbers > 190 in Figure 9) and the warm core ring (entry numbers 150–225 in Figure 10), $[L_w(\lambda)]_N$ in all three bands increases and decreases simultaneously, again suggesting that the variations are due to variations in scattering. However, in contrast to the image in Plate 1, the radiances in the bright areas where the two tracks intersect are significantly larger than can be explained on the basis of the model, i.e., a value of $b^0 > 0.45$ m^{-1} is required to produce the high values of $[L_w(\lambda)]_N$ at 520 and 550 nm. In fact, $b^0 > 1$ m^{-1} is required by the model to yield an $[L_w(\lambda)]_N$ at 550 nm of 1 mW cm^{-2} μm sr at a pigment concentration of
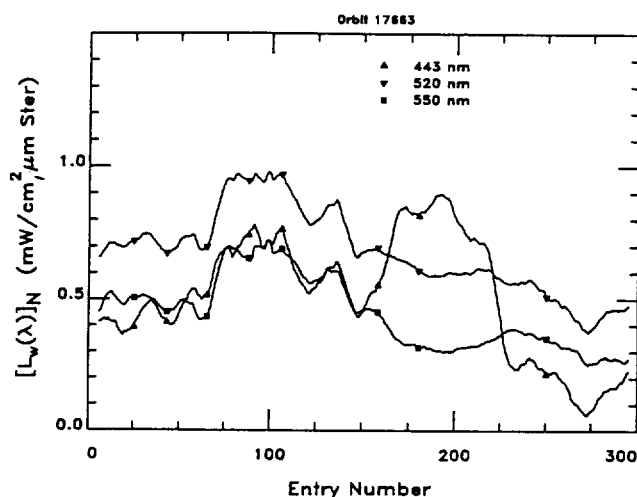

Fig. 10. Extracted values of $[L_w(443)]_N$, $[L_w(520)]_N$, and $[L_w(550)]_N$ along the green track in Plate 2.

1 mg m^{-3}, far in excess of that allowed for Case 1 waters [*Gordon and Morel*, 1983]. The bright areas in these images are known to have been populated by blooms of the coccolithophroid *Emiliana huxleyi* (P. Blackwelder, unpublished data, 1982). These cells are covered with scales (called coccoliths) which become detached and can reach concentrations 10–20 times that of the cells themselves. Although this phenomenon of scale detachment apparently does not occur in laboratory-cultured suspensions of coccolithophorid cells, coccoliths have been studied in the field using CZCS imagery [*Holligan et al.*, 1983] and are characterized by extraordinarily high backscattered solar radiance. Unfortunately, there appears to be little or no correlation between the concentration of detached coccoliths and *E. huxleyi* cells, i.e., the pigment concentration. *Bricaud et al.* [1983a] have shown that laboratory cultures of *E. huxleyi* also possess strong scattering compared to other species of phytoplankton, but this is a characteristic of the cells themselves, not detached coccoliths. The high reflectance of the water is believed to be due to the presence of these coccolithophorid blooms, which include cells and detached coccoliths. The introduction of this additional component, detached coccoliths, necessitates a modification of the model and the introduction of at least one other parameter. It also poses a problem in the definition of Case 1 waters, since a portion of the high scattering is due to the detached coccoliths, which do not covary with *C*. However, since the optical properties of the water are controlled principally by phytoplankton and their associated detrital material, the coccoliths, it meets all the formal criteria for classification as Case 1. We suggest that these waters be classified as Case 1 regardless of their high scattering; however, it must be realized that the Morel Case 1–Case 2 classification [*Morel and Prieur*, 1977] can no longer be made solely on the basis of the remotely determined optical properties alone; the physical setting in which the observations are made must also be considered.

Considering the possible impact of detached coccoliths on the flux of carbon out of the euphotic zone in the oceans, a goal of ocean color remote sensing must be an estimation of their concentration. Also, since their presence interferes with remote estimates of the pigment concentration, another goal must be the appropriate modification of bio-optical algorithms for application to coccolithophore blooms. Both goals require detailed knowledge of the inherent optical properties of the detached coccoliths. Application of the present model for estimating the relevant optical properties is described later in this paper.

Effect of Yellow Substances

Finally, we consider the influence of YS fluctuations over and above the "background" level, which we hypothesize to be already included in K_c, on $[L_w(\lambda)]_N$. Figures 11, 12, and 13 show the effect of these YS on $[L_w(\lambda)]_N$ for $b^0 = 0.3$ mg m^{-3} and YS concentrations, $C_{YS} \equiv a_{ys}(375) - 0.06$ m^{-1}, of 0, 0.012, 0.024, 0.036, 0.048, and 0.060 m^{-1}. As expected, the added

Fig. 12. The radiance $[L_w(520)]_N$ as a function of the pigment and YS concentrations. The curves are the results of the model, with $b^0 = 0.30$ m^{-1}, and different curves correspond to different concentrations of YS. From top to bottom, the curves correspond to $C_{ys} \equiv a_{ys}(375) - 0.06$ m^{-1}, of 0, 0.012, 0.024, 0.036, 0.048, and 0.06 m^{-1}. The points are *Clark*'s [1981] experimental measurements.
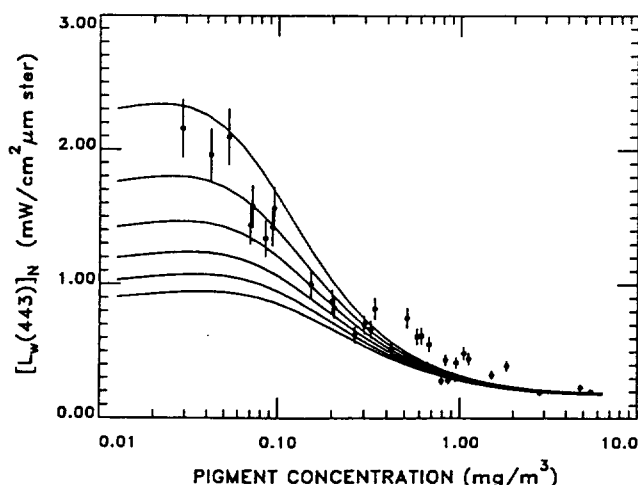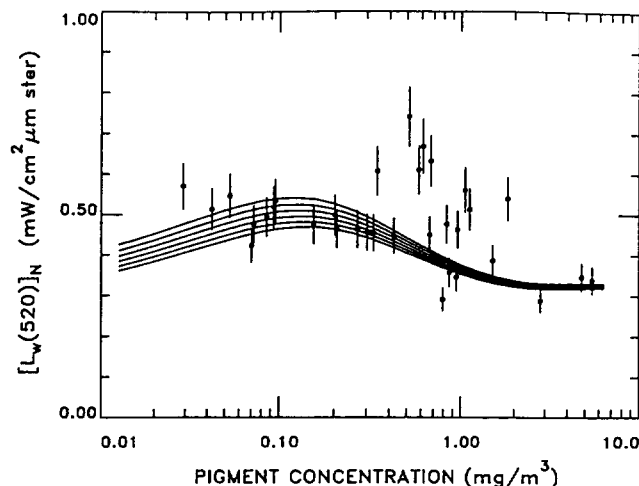

Fig. 11. Value of $[L_w(443)]_N$ as a function of the pigment and yellow substances (YS) concentrations. The curves are the results of the model, with $b^0 = 0.30$ m^{-1}, and different curves correspond to different concentrations of YS. From top to bottom, the curves correspond to $C_{ys} \equiv a_{ys}(375) - 0.06$ m^{-1}, of 0, 0.012, 0.024, 0.036, 0.048, and 0.06 m^{-1}. The points are *Clark*'s [1981] experimental measurements.
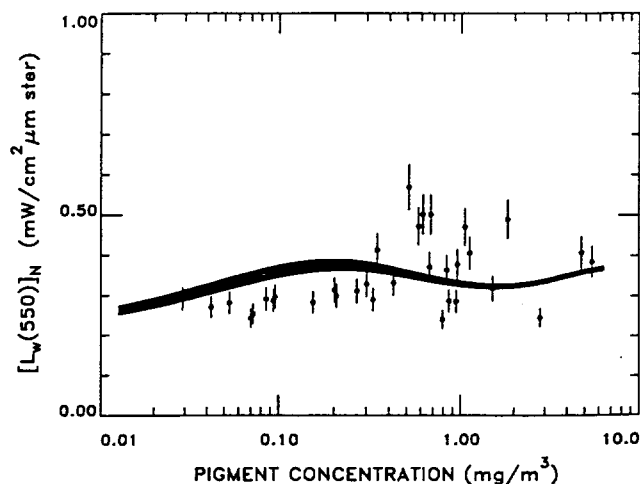

Fig. 13. The radiance $[L_w(550)]_N$ as a function of the pigment and YS concentrations. The curves are the results of the model, with $b^0 = 0.30$ m^{-1}, and different curves correspond to different concentrations of YS. From top to bottom, the curves correspond to $C_{ys} \equiv a_{ys}(375) - 0.06$ m^{-1}, of 0, 0.012, 0.024, 0.036, 0.048, and 0.06 m^{-1}. The points are *Clark*'s [1981] experimental measurements.
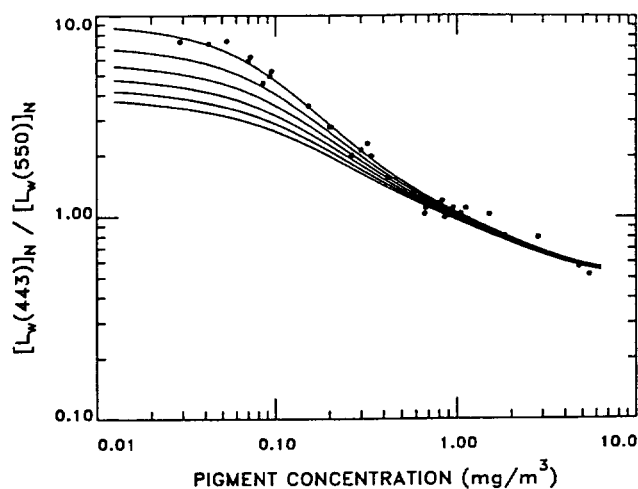
Fig. 14. The radiance ratio $[L_w(443)_N/[L_w(550)]_N$ as a function of the pigment and YS concentrations. The curves are the result of the model with $b^0 = 0.20$ m^{-1}., and different curves correspond to different concentrations of YS. From top to bottom, the curves correspond to $C_{ys} \equiv a_{ys}(375) - 0.06$ m^{-1}, of 0, 0.012, 0.024, 0.036, 0.048, and 0.06 m^{-1}. The points are Clark's [1981] experimental measurements.

absorption decreases the radiance at all wavelengths, but because of its exponential spectral variation the decrease is far more pronounced in the blue than in the green. Clearly, the data at 520 and 550 nm do not favor any particular value of the YS concentration; however, the data at 443 nm obviously favor C_{ys} values near zero. In fact, the three data points with the lowest pigment concentrations were obtained in the Sargasso Sea, an area virtually free of dissolved organic material [Bricaud et al., 1983b], and hence it is to be expected that $C_{ys} = 0$ would be appropriate for this data. (Recall that the Baker and Smith [1982] K values for low C were also measured in the Sargasso Sea, and they are therefore free of any background YS) For the rest of the data it is difficult to separate the effects of varying YS from varying b^0. However, it can be accomplished by recalling that the variance due to b^0 variations (which are expected to be approximately the same at each wavelength) is strongly reduced when radiance ratios are formed, while the effect of YS on the ratios must be large because of the strong spectral character of its absorption. In Figure 14 the blue-green radiance ratio is compared with the experimental data, using the optimized values of $b^0(443)$ and $b^0(550)$ and C_{ys} values from Figures 11, 12, and 13. It is clear that this data set favors a negligible amount of YS above the background level, when $C \leq 0.2$ mg m^{-3}, and that for larger values of C only a modest amount of the fluctuating YS component is required to explain much of the "noise" in the ratio. At high values of C (≥ 0.5 mg m^{-3}) the fluctuating YS component is seen to have very little influence on the blue-green ratio. Furthermore, at this higher pigment level the fluctuating component has very little effect on the actual radiances themselves. In fact, the YS effect is less than that induced by a change in b^0 of ± 0.1 m^{-1} at 443 nm and is significantly less at 550 nm. Thus for this data set, YS fluctuating over the background value would not interfere with the determination of b^0 for classification of the scattering properties of phytoplankton and their associated detrital material described earlier. It must be remembered, however, that the YS concentrations used here are representative of oceanic areas only. In coastal regions the concentration can be much higher, with

$a_{ys}(375)$ reaching an order of magnitude or more than the maximum concentration considered here ($a_{ys}(375) = 0.06$ m^{-1} above background). For such high concentrations the sensitivity of $[L_w(\lambda)]_N$ to variations in C clearly will be negligible, and retrieval of C from radiance measurements will be difficult if not impossible.

APPLICATIONS

Bio-optical Algorithm Improvement

An obvious application of the current work is the replacement of the standard bio-optical algorithm (i.e., a linear fit to Clark's [1981] data in Figure 6) by the model result, which provides a somewhat better fit to the data, particularly for $C > 1$ mg m^{-3}. The model can also serve to identify and interpret deviations from Case 1 waters by comparison of satellite-derived radiance with the model results.

Atmospheric Correction Improvement

Figure 3 shows that for $b^0 \approx 0.2$ m^{-1} the model reasonably well reproduces the minimum $[L_w(550)]_N$ observed for a given C. Furthermore, this minimum $[L_w(550)]_N$ is seen to be only weakly dependent on C over the range $0.01 < C < 10$ mg m^{-3}. The total variation in the minimum $[L_w(550)]_N$ is from 0.26 to 0.32 mW cm^{-2} μm sr, or approximately a spread of 2.4 CZCS DC. This observation can be used to aid in the atmospheric correction of CZCS imagery. As described in the appendix, the atmospheric correction parameters, $\varepsilon(\lambda_2, \lambda_1)$, are presently determined by locating clear water ($C < 0.25$ mg m^{-3}) in the image for which Clark's [1981] data show that $[L_w(520)]_N$ and $[L_w(550)]_N$ are nearly independent of C (Figures 2 and 3). Thus $[L_w(\lambda)]_N$ is known for $\lambda = 520, 550,$ and 670 nm, and this allows the estimation of $\varepsilon(520, 670)$ and $\varepsilon(550, 670)$. Then $\varepsilon(443, 670)$ is determined by extrapolation. These ε values are then used for the entire scene or subscene. There are several problems with this procedure. First, there may be no clear water in the scene or subscene of interest. Next, the character of the aerosol may change over the region of interest, and this changes the ε. Finally, even in an atmosphere containing an aerosol with horizontally constant optical properties, the ε have been shown to vary with position. Thus it is important to have many determinations of ε over the region of interest, but this is usually impossible because of the typically poor distribution of clear-water pixels. One can use the present model, however, to compute $\varepsilon(550, 670)$ at each pixel from the minimum $[L_w(550)]_N$, which, as discussed earlier, is nearly independent of C. This field of $\varepsilon(520, 670)$ values is incorrect because we have assumed that $[L_w(550)]_N$ is equal to its minimum value everywhere in the scene. It is reasonable to expect, however, that $[L_w(550)]_N$ is equal to its minimum value at a few, hopefully well-distributed, positions in the scene, even when $C > 0.25$ mg m^{-3}. Assuming that $[L_w(670)]_N \approx 0$ everywhere (which can be verified by looking for oceanlike structure in the $L_a(670)$ field), the resulting field of minimum values of $\varepsilon(550, 670)$ can be expected to be correct. The higher values are rejected, since they were derived from pixels where $[L_w(550)]_N$ was greater than the minimum, with the residual interpreted as an addition to $L_a(550)$ which increases $\varepsilon(550, 670)$. By interpreting the field of minimum ε values it should be possible to derive $\varepsilon(550, 670)$ at each pixel and, by extrapolation, $\varepsilon(520, 670)$ and $\varepsilon(443, 670)$. Such a procedure has the potential for considerably increasing the accuracy of atmospheric corrections.

Improved Bio-optical Algorithms in the Presence of Coccolithophorids

The standard bio-optical algorithms are known to systematically underestimate the pigment concentration in blooms of the coccolithopore *E. Huxleyi*. Unlike typical oceanic regions at high pigment concentrations, where the water-leaving radiance in the blue is too small to be useful, all of the water-leaving radiances are high in these coccolithophore blooms, even at high pigment concentrations. Thus the blue-green ratio can potentially be used to estimate C in such blooms. As described earlier, the addition of the coccolith component to our radiance model requires the optical properties of the coccoliths. Since direct measurements of these optical properties have yet to be made, they must be estimated indirectly.

Viollier and Sturm [1984] have estimated the reflectance $R(\lambda)$ as a function of wavelength across a coccolithophore bloom, using CZCS imagery. Several spectra were presented for a region where the pigment concentration was known to range from 0.5 to 3.0 mg m^{-3} and the number of coccolithophorid cells ranged from 0 to 8000 mL^{-1}; however, the pigment and cell concentrations for the individual spectra were not provided. The $R(\lambda)$ values varied from those typical of oceanic-coastal waters, e.g., less than 0.03–0.04 at 443 nm, to extraordinarily high values, e.g., nearly 0.18. The high values are believed to result from the scattering of detached coccoliths. Since detached coccoliths tend to increase $R(\lambda)$, while pigments tend to decrease $R(\lambda)$, further information is required to separate the effects of these two components. However, the semianalytic model presented previously can be used to provide bounds on the optical properties of the detached coccoliths, if we assume they are well-mixed near the surface. *Gordon et al.* [1975] show that for a homogeneous ocean the quantity

$$X \equiv \frac{b_b}{a + b_b}$$

can be directly determined from R according to

$$X = -0.0003 + 3.077R - 4.216R^2 + 3.501R^3 \qquad (13)$$

As before, we use (3') to relate K to $a + b_b$; however, since the detached coccoliths are calcium carbonate and therefore nonabsorbing, b_f/c will be nearly unity for this component. Thus for the high reflectance found by *Viollier and Sturm* [1984] we choose $\kappa_1 = 1.083$, i.e., the large b_f/c linear approximation to K (equation (3')). The addition of nonabsorbing detached coccoliths to the previous model then simply requires

$$(b_b)_w + (b_b)_p \rightarrow (b_b)_w + (b_b)_p + (b_b)_{cc}$$

and

$$a_w + a_p + (b_b)_w + (b_b)_p = \frac{K}{D_0\kappa_1} \rightarrow \frac{K}{D_0\kappa_1} + (b_b)_{cc}$$

so X in (13) becomes

$$X = \frac{(b_b)_w + (b_b)_p + (b_b)_{cc}}{K/D_0\kappa_1 + (b_b)_{cc}}$$

where $(b_b)_{cc}$ is the backscattering coefficient of the coccoliths. Given the pigment concentration, (13) can be inverted to find $(b_b)_{cc}$. Since C is known to fall within $0.5 \le C \le 3.0$ mg m^{-3}, we can compute $(b_b)_{cc}$ as a function of C, providing a range of estimates for $(b_b)_{cc}$. As in the model without coccoliths, D_0 was chosen to be 1.1. We then formed the ratio of $(b_b)_{cc}$ at λ to 550

nm,

$$r_{cc}(\lambda) = \frac{[b_b(\lambda)]_{cc}}{[b_b(550)]_{cc}}$$

Because the reflectance at 443 nm is sensitive to the pigment concentration, $r_{cc}(443)$ is examined. The range of variation of $r_{cc}(443)$, consistent with the known pigment range, is found to be

$$1.75 \le r_{cc}(443) \le 2.36$$

i.e., for each spectrum it is possible to find a value of C between 0.5 and 3.0 mg m^{-3} that will yield $r_{cc}(443)$ in this range. Since all detached coccoliths in a given bloom are presumably similar, $r_{cc}(\lambda)$ must be the same for all reflection spectra. Thus variation in $R(\lambda)$ from location to location should be completely explained by variation in C and the concentration of coccoliths.

It is not possible to sharpen the estimate of $r_{cc}(443)$ without further data; however, we believe that $r_{cc}(443)$ is closer to 1.75 than to 2.36. This is based on the fact that $r_{cc}(443)$ would be only 2.44 for particles completely within the Rayleigh scattering regime, i.e., particle size much less than λ; however, the disk-shaped coccoliths have diameters of several wavelengths. Also, the *Viollier and Sturm* [1984] retrieval method would be most accurate for spectra with high overall reflectivity. For these spectra the lower pigment concentrations ($0.5 \le C \le 1.0$ mg m^{-3}) provided $r_{cc}(443)$ in the range 1.75–2.0. It seems reasonable that the spectra with the highest reflectance at 443 nm should be associated with lower pigment concentrations, and this also favors the lower values of $r_{cc}(443)$. We model the coccolith backscattering by assuming a power law variation in wavelength, i.e.,

$$[b_b(\lambda)]_{cc} = B_{cc}\left(\frac{550}{\lambda}\right)^n$$

where B_{cc} is a constant proportional to the concentration of coccoliths and n is a constant. Taking $n = 2.5$–3 yields $r_{cc}(443) = 1.75$–1.95. These values for n also provide values of $r_{cc}(520)$ in the range determined from $R(\lambda)$, in the same manner as $r_{cc}(443)$.

Incorporation of detached coccoliths into our radiance model is difficult because of the number of parameters required. We want to use the blue-green ratio to estimate C in coccolithophore blooms because (1) there is sufficient blue light to form the ratio even at high pigment concentrations, and (2) this ratio is far more sensitive to C than the 520–550 ratio (Figure 7). However, this means that there are only two pieces of data, $[L_w(443)]_N$ and $[L_w(550)]_N$, available to estimate four parameters: C, b^0, B_{cc}, and n. We therefore have to fix two of the parameters. The exponent n is relatiely easy to estimate, based on our earlier analysis, and we set $n = 2.5$. The difficult problem, however, is the division of the scattering between b^0 and B_{cc}. Clearly, not all of the variance in backscattering can be due to B_{cc}. However, to find at least a qualitative picture of the effect of B_{cc} on $[L_w(\lambda)]_N$, we essentially assume that the variance is due to B_{cc} and set $b^0 = 0.2$ m^{-1}. This value reproduces $[L_w(550)]_N$ for low pigment concentrations and provides a reasonable estimate for the smallest backscattering for a given C. Figures 15, 16, and 17 show model computations, of $[L_w(443)]_N$, $[L_w(550)]_N$, and their ratio, respectively, as a function of B_{cc} and C. Again, the computations are superimposed over *Clark*'s [1981] direct measurements. (At 443 nm the $i > 1$ term in equation (2) be-
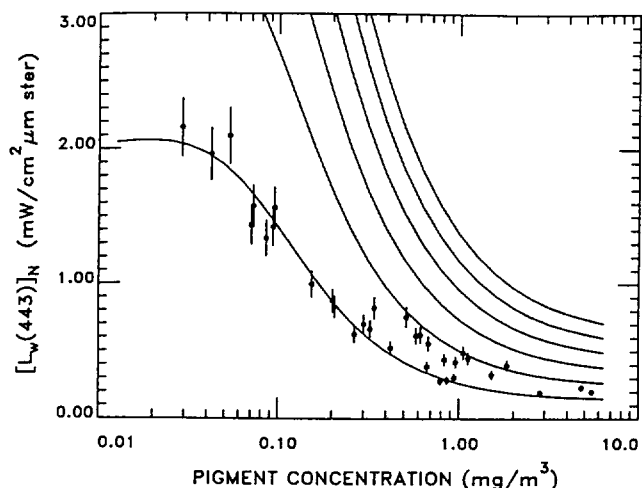
Fig. 15. The radiance $[L_w(443)]_N$ as a function the pigment and detached coccolith concentrations. The curves are the results of the model, with $b^0 = 0.20$ m^{-1}, and different curves correspond to different concentrations of detached coccoliths. From top to bottom, the curves correspond to B_{cc} of 0.0125, 0.0100, 0.0075, 0.0050, and 0 m^{-1}. The points are *Clark's* [1981] experimental measurements.
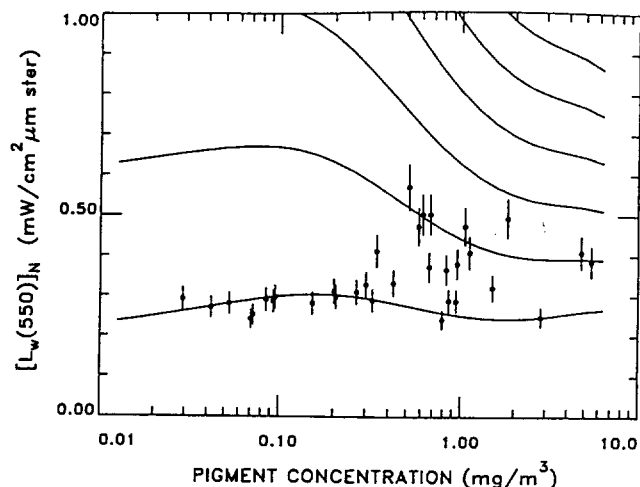

Fig. 16. The radiance $[L_w(550)]_N$ as a function of the pigment and detached coccolith concentrations. The curves are the results of the model, with $b^0 = 0.20$ m^{-1}, and different curves correspond to different concentrations of detached coccoliths. From top to bottom, the curves correspond to B_{cc} of 0.0125, 0.0100, 0.0075, 0.0050, 0.0025, and 0 m^{-1}. The points are *Clark's* [1981] experimental measurements.

comes important (the error caused by its omission is $\gtrsim 20\%$), when $[L_w]_N \gtrsim 2.5$ mW cm^{-2} μm sr, thus the model computations in Figure 15 become inaccurate for water radiances greater than about 2.5 mW cm^{-2} μm sr.) Several observations from these computations are pertinent. First, for high pigment concentrations, i.e., greater than about 2 mg m^{-3}, the variation of $[L_w(\lambda)]_N$ with the coccolith concentration (B_{cc}) is roughly the same for each band. Thus the added radiance due to the coccoliths appears to be white at high pigment concentrations. Assuming that the pigment concentrations in the brightest areas in Plate 2 are greater than 2 mg m^{-3}, Figures 15 and 16 suggest that they correspond to $B_{cc} \approx 0.01$ m^{-1}. Since b^0 was chosen near its lower limit, these data suggest that $B_{cc} < 0.01$ m^{-1} for the Middle Atlantic Bight in April 1982. Since the backscattering probability associated with the coccoliths is unknown, an upper limit cannot be placed on their total scattering. Second, the effect of the coccoliths on the blue-green ratio for estimating C (Figure 17) is in the right direction, i.e., for a given value of the ratio the pigment concentration will be underestimated for $C > 0.3$ mg m^{-3} when the presence of the coccoliths is ignored. Third, the modified model can be used to provide an improved estimate of C, even though the value of b^0 used in the model is probably incorrect. This estimate would be developed by first estimating C, assuming that $B_{cc} = 0$, and then using the model to predict the expected radiance at 550 nm. The difference between the actual radiance and the expected radiance based on the model and the estimated value of C is formed and used with Figure 16 to estimate B_{cc}. This value of B_{cc} is then used to derive the "corrected" blue-green pigment algorithm, which will yield an improved estimate of C. Figure 17 shows the blue-green ratio to be most sensitive to the value of B_{cc} for low values, i.e., $0 \leq B_{cc} \leq 0.0025$ m^{-1}, while for $B_{cc} > 0.005$ m^{-1}, variations in B_{cc} yield relatively small changes in C. Thus if the corrected algorithm is used only for large B_{cc}, e.g., $B_{cc} > 0.005$ m^{-1}, a significant improvement will result even though the value of b^0 is incorrect. Conversely, the concentration of coccoliths is proportional to B_{cc}, and estimation of this depends strongly on b^0. For example, Figures 3 and 16 show that for $C > 0.3$ mg m^{-3}, $b^0 = 0.2$ m^{-1} and $B_{cc} = 0.0025$ m^{-1} produce roughly the same $[L_w(550)]_N - C$ relationship as $b^0 = 0.45$ m^{-1} and $B_{cc} = 0$. Thus this procedure can produce an error in B_{cc} of as much as 0.0025 m^{-1}.

This model of the influence of detached coccoliths from *E. Huxleyi* on $[L_w(\lambda)]_N$ is not presented as a proven scheme for analysis of CZCS imagery. In fact, the choice of the model parameters, in particular n, may be inappropriate for other species of coccolithophores or in instances in which the coccoliths are not detached from the host cells [*Balsh et al.*, 1987]. Rather, it is presented as a likely candidate for an approach that deserves further research. We believe this approach can be "tuned" using existing measurements in the Middle Atlantic Bight, and we are in the process of attempting this.

SUMMARY AND CONCLUSIONS

We have presented a model of ocean color which relates the normalized water-leaving radiance to the pigment concentration for Morel Case 1 waters. In the simplest case only one additional parameter (b^0) is needed. Direct measurements of b^0 reveal a variation by about a factor of 4, which is sufficient to explain nearly all of the variance in surface measure-
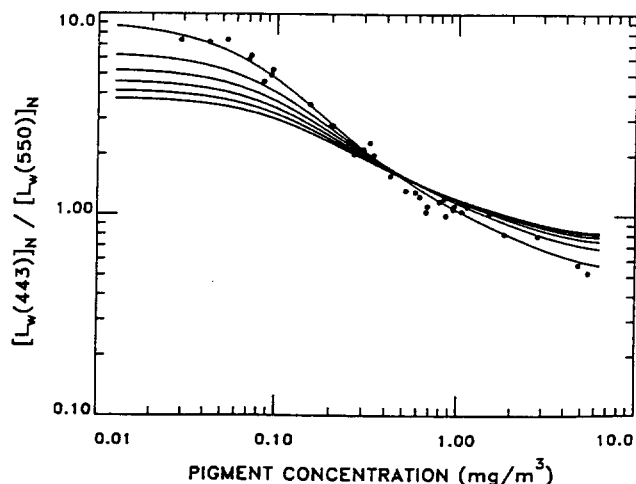

Fig. 17. The radiance ratio $[L_w(443)]_N/[L_w(550)]_N$ as a function of the pigment and detached coccolith concentrations. The curves are the results of the model, with $b^0 = 0.20$ m^{-1}, and different curves correspond to different concentrations of detached coccoliths. From top to bottom at the right edge of the graph, the curves correspond to B_{cc} of 0.0125, 0.0100, 0.0075, 0.0050, 0.0025, and 0 m^{-1}. The points are *Clark's* [1981] experimental measurements.

ments of the $[L_w(\lambda)]_N - C$ relationship. The model provides an excellent fit to the blue-green ratio as a function of C for all values of b^0 that fall within the acceptable range for Case 1 waters. This explains the considerable reduction of variance seen in the radiance ratios compared to the radiances themselves. Variance similar to surface measurements is also observed in CZCS imagery; however, situations are found which require values of b^0 to be too large for the water to be classified as Case 1, even though no Case 2 contaminants are believed to be present, i.e., the optical properties of the water are still controlled by phytoplankton and their immediate detritus. In the cases examined, the apparently large values required for b^0 were believed to be due to enhanced scattering by detached coccoliths from the coccolithophorid *Emiliana huxleyi*. The optical properties of the detached coccoliths are estimated from reflectance measurements, and the radiance model is modified to include their effects. The expanded model suggests the possibility of estimating the coccolith concentration. It explains the observation that the pigment concentrations retrieved by CZCS in *E. Huxleyi* blooms are generally too low.

The original purpose of developing the model was to improve atmospheric correction by providing $[L_w(\lambda)]_N$ at moderate to high pigment concentrations. To this end, an important result of the model is that the minimum $[L_w(550)]_N$ for a given C is approximately independent of C. This can be used to extend the "clear-water radiance" concept to high pigment concentrations, providing a field of atmospheric correction parameters which have the property that low-pass filtering their minimum values can provide an estimate of the correction parameters for each individual pixel. Direct application of these ideas, along with the model, to CZCS imagery is currently underway.

Finally, the excellent agreement between the model and the surface measurements for waters from several locations provides strong evidence that the blue-green ratio in Figure 6 can be considered a universally applicable algorithm for estimating C in Case 1 waters that are free of YS and optically vigorous debris such as detached coccoliths.

APPENDIX: CZCS ATMOSPHERIC CORRECTION

Present CZCS atmospheric correction techniques [*Gordon*, 1978; *Gordon and Clark*, 1980, 1981; *Gordon et al.*, 1983b; *Smith and Wilson*, 1981] utilize the fact that in the open ocean, over some range of pigment concentration, the radiance leaving the ocean (water-leaving radiance) can be predicted with high accuracy. At low to moderate concentrations the ocean appears as almost a blackbody in the red (670 nm), and at low concentrations the water-leaving radiance in the green (520 nm) and yellow (550 nm) bands is found to be nearly independent of the concentration. Briefly, the sensor radiance at a wavelength λ, $L_t(\lambda)$, is divided into its components: $L_r(\lambda)$, the contribution arising from Rayleigh scattering, $L_a(\lambda)$, the contribution arising from aerosol scattering, and $t(\lambda)L_w(\lambda)$, the inherent sea surface radiance diffusely transmitted to the top of the atmosphere, i.e.,

$$L_t(\lambda) = L_r(\lambda) + L_a(\lambda) + t(\lambda)L_w(\lambda) \qquad (A1)$$

where t is the diffuse transmittance of the atmosphere. L_a and L_r include the contribution of sky light specularly reflected from the sea surface, but not the specularly reflected solar beam (Sun glitter) which is avoided by tilting the instrument away from the reflected image of the Sun. Since $L_r(\lambda)$ and $t(\lambda)$ can be computed from known properties of the atmosphere [*Gordon et al.*, 1983b; 1988], given $L_w(\lambda)$ in two spectral bands

at one position, $L_a(\lambda)$ can be found there from (A1), and the ratio

$$S(\lambda_2, \lambda_1) = \frac{L_a(\lambda_2)}{L_a(\lambda_1)} \qquad (A2)$$

can then be formed. When the aerosol scattering phase function is approximately independent of wavelength, the single scattering approximation shows that S is related to the optical properties of the atmosphere through

$$S(\lambda_2, \lambda_1) = \varepsilon(\lambda_2, \lambda_1)\frac{F'(\lambda_2)}{F'(\lambda_1)} \qquad (A3)$$

where $F'(\lambda_2)$ and $F'(\lambda_1)$ are the extraterrestrial solar irradiances at λ_2 and λ_1, respectively, reduced by two trips through the ozone layer, and $\varepsilon(\lambda_2, \lambda_1)$ is the ratio of the aerosol optical thicknesses at λ_2 and λ_1. The $\varepsilon(\lambda_2, \lambda_1)$ factors are called the atmospheric correction parameters. They depend only on the normalized size distribution and refractive index of the aerosol and not on its concentration. Thus in an atmosphere in which the aerosol variations are limited to variations in concentration only, ε remains constant, independent of horizontal position (even though both $L_a(\lambda_2)$ and $L_a(\lambda_1)$ may vary individually). Using (A2) and (A3), (A1) becomes

$$L_w(\lambda_2) = [t(\lambda_2)]^{-1}\{L_t(\lambda_2) - L_r(\lambda_2) - \varepsilon(\lambda_2, \lambda_1)[F'(\lambda_2)/F'(\lambda_1)]$$
$$\cdot [L_t(\lambda_1) - L_r(\lambda_1) - t(\lambda_1)L_w(\lambda_1)]\} \qquad (A4)$$

The specific application of this formula to CZCS is based on the "clear-water radiance" concept [*Gordon and Clark*, 1981], which provides $L_w(\lambda)$ at 520, 550, and 670 nm when the pigment concentration is less than 0.25 mg m^{-3}. Equations (A1) through (A3) are then used to find the correction factors $\varepsilon(520, 670)$, $\varepsilon(550, 670)$, and $\varepsilon(670, 670)$ at pixels with $C < 0.25$ mg m^{-3}. Then $\varepsilon(443, 670)$ is found by extrapolation. This enables determination of all of the atmospheric correction parameters over such regions, and these parameters are then assumed to be applicable to the whole image. In this procedure it is assumed that $L_w(670) = 0$. Thus taking λ_1 to be 670 nm, (A4) provides L_w at each of the other three wavelengths (λ_2). For regions where the pigment concentration is sufficiently high that the ocean is not a blackbody in the red, an empirical relationship concerning the spectral composition of the water-leaving radiance is used to provide the radiance in the red [*Austin and Petzold*, 1981], and the resulting system of equations is solved by iteration [*Smith and Wilson*, 1981]. These procedures work well as long as the atmospheric correction parameters are constant over the image: a criterion which is reasonably well satisfied for small subscenes of a full CZCS image if the aerosol type, e.g., continental, marine, or a particular mixture of the two, remains the same over the subscene. However, *Gordon and Castaño* [1987] have shown that even when this criterion is satisfied for a full image, multiple scattering produces a residual variation in $\varepsilon(\lambda_2, \lambda_1)$ across the individual scan lines. Also, variations in the aerosol type often occur in particular images of waters near continental land masses. Thus it is desirable to be able to determine the atmospheric correction parameters at each individual pixel, or at least at a large enough number of pixels to be able to remove the low spatial frequency variations in these parameters.

REFERENCES

Austin, R. W., The remote sensing of spectral radiance from below the ocean surface, in *Optical Aspects of Oceanography*, edited by N. G. Jerlov and E. S. Nielsen, pp. 317–344, Academic, San Diego, Calif., 1974.

Austin, R. W., Coastal zone color scanner radiometry, Ocean Optics VI, *Proc. Soc. Photo Opt. Instrum. Eng.*, *208*, 170–177, 1979.

Austin, R. W., and T. J. Petzold, Remote sensing of the diffuse attenuation coefficient of sea water using the coastal zone color scanner, in *Oceanography From Space*, edited by J. R. F. Gower, pp. 239–256, Plenum, New York, 1981.

Baker, K. S., and R. C. Smith, Bio-optical classification and model of natural waters, 2, *Limnol. Oceanogr.*, *27*, 500–509, 1982.

Balsh, W. M., M. Abbott, R. Eppley, and F. Reid, The effect of coccolithophorids on the remote sensing of chlorophyll and primary productivity from space, *Eos Trans. AGU*, *68*, 1703, 1987.

Bricaud, A., A. Morel, and L. Preiur, Optical efficiency factors of some phytoplankters, *Limnol. Oceanogr.*, *28*, 816–832, 1983a.

Bricaud, A., A. Morel, and L. Preiur, Absorption by dissolved organic matter in the sea (yellow substance) in the UV and visible domains, *Limnol. Oceanogr.*, *26*, 43–53, 1983b.

Brown, O. B., R. H. Evans, J. W. Brown, H. R. Gordon, R. C. Smith and K. S. Baker, Phytoplankton blooming of the U.S. east coast: A satellite description, *Science*, *229*, 163–167, 1985.

Carder, K. L., R. G. Steward, and P. R. Payne, Solid-state spectral transmissometer and radiometer, *Opt. Eng.*, *24*, 863–868, 1985.

Carder, K. L., D. J. Collins, M. J. Perry, H. L. Clark, J. M. Mesias, J. S. Cleveland and J. Greenier, The interaction of light with phytoplankton in the marine environment, Ocean Optics VII, *Proc. SPIE, Int. Soc. Opt. Eng.*, *637*, 42–55, 1986a.

Carder, K. L., R. G. Steward, J. H. Paul, and G. A. Vargo, Relationships between chlorophyll and ocean color constituents as they affect remote-sensing radiance models, *Limnol. Oceanogr.*, *31*, 403–413, 1986b.

Clark, D. K., Phytoplankton algorithms for the Nimbus 7 CZCS, in *Oceanography From Space* edited by J. R. F. Gower, pp. 227–238, Plenum, New York, 1981.

Gordon, H. R., Radiative transfer in the ocean: A method for determination of absorption and scattering properties, *Appl. Opt.*, *15*, 2611–2613, 1976.

Gordon, H. R., Removal of atmospheric effects from satellite imagery of the oceans, *Appl. Opt.*, *17*, 1631–1636, 1978.

Gordon, H. R., Ocean color remote sensing: Influence of the particle phase function and the solar zenith angle., *Eos Trans. AGU*, *14*, 1055, 1986.

Gordon, H. R., and D. J. Castaño, The coastal zone color scanner atmospheric correction algorithm: Multiple scattering effects, *Appl. Opt.*, *26*, 2111–2122, 1987.

Gordon, H. R., and D. K. Clark, Atmospheric effects in the remote sensing of phytoplankton pigments, *Boundary Layer Meteorol.*, *18*, 299–313, 1980.

Gordon, H. R., and D. K. Clark, Clear water radiances for atmospheric correction of coastal zone color scanner imagery, *Appl. Opt.*, *20*, 4175–4180, 1981.

Gordon, H. R., and A. Y. Morel, *Remote Assessment of Ocean Color for Interpretation of Satellite Visible Imagery: A Review*, 114 pp., Springer-Verlag, New York, 1983.

Gordon, H. R., O. B. Brown, and M. M. Jacobs, Computed relationships between the inherent and apparent optical properties of a flat homogeneous ocean, *Appl. Opt.*, *14*, 417–427, 1975.

Gordon, H. R., D. K. Clark, J. L. Mueller, and W. A. Hovis, Phytoplankton pigments derived from the Nimbus 7 CZCS: Initial comparisons with surface measurements, *Science*, *210*, 63–66, 1980.

Gordon, H. R., J. W. Brown, O. B. Brown, R. H. Evans and D. K. Clark, Nimbus 7 coastal zone color scanner: Reduction of its radiometric sensitivity with time, *Appl. Opt.*, *22*, 3929–3931, 1983a.

Gordon, H. R., D. K. Clark, J. W. Brown, O. B. Brown, R. H. Evans, and W. W. Broenkow, Phytoplankton pigment concentrations in the Middle Atlantic Bight: Comparison between ship determinations and coastal zone color scanner estimates, *Appl. Opt.*, *22*, 20–36, 1983b.

Gordon, H. R., J. W. Brown, and R. H. Evans, Exact Rayleigh Scattering calculations for use with the Nimbus 7 coastal zone color scanner, *Appl. Opt.*, *27*, 862–871, 1988.

Hobson, L. A., D. W. Menzel, and R. T. Barber, Primary productivity and the sizes of pools of organic carbon in the mixed layer of the ocean, *Mar. Biol.*, *19*, 298–306, 1973.

Holligan, P. M., M. Viollier, D. S. Harbour, P. Camus, and M. Champagne-Philippe, Satellite and ship studies of coccolithophore production along the continental shelf edge, *Nature*, *304*, 339–342, 1983.

Hovis, W. A., et al., Nimbus 7 coastal zone color scanner: System description and initial imagery, *Science*, *210*, 60–63, 1980.

Morel, A., Optical Properties of pure water and pure sea water, in *Optical Aspects of Oceanography*, edited by N. G. Jerlov and E. S. Nielsen, pp. 1–24, Academic, San Diego, Calif., 1974.

Morel, A., In-water and remote measurement of ocean color, *Boundary Layer Meteorol.*, *18*, 177–201, 1980.

Morel, A., and A. Bricaud, Theoretical results concerning light absorption in a discrete medium, and application to specific absorption of phytoplankton, *Deep Sea Res.*, *28A*, 1375–1393, 1981.

Morel, A., and H. R. Gordon, Report of the working group on ocean color, *Boundary Layer Meteorol.*, *18*, 343–355., 1980.

Morel, A., and L. Prieur, Analysis of variations in ocean color, *Limnol. Oceanog.*, *22*, 709–722, 1977.

Plass, G. N., G. W. Kattawar, and J. A. Guinn, Radiative transfer in the Earth's atmosphere: Influence of ocean waves, *Appl. Opt.*, *14*, 1924–1936, 1975.

Preisendorfer, R. W., Application of radiative transfer theory to light measurements in the sea, *Monogr. 10*, pp. 11–30, Int. Union Géod. Geophys., Paris, 1961.

Preisendorfer, R. W., *Radiative Transfer on Discrete Spaces*, 462 pp., Pergamon, Oxford, 1965.

Preisendorfer, R. W., and C. D. Mobley, Albedos and glitter patterns of a wind-roughened sea surface, *J. Phys. Oceanogr.*, *16*, 1293–1316, 1986.

Prieur, L., and S. Sathyendranath, An optical classification of coastal and oceanic waters based on the specific absorption curves of phytoplankton pigments, dissolved organic matter, and other particulate materials, *Limnol. Oceanogr.*, *26*, 671–689, 1981.

Sathyendranath, S., Influence des substances en solution et en suspension dans les eaux de mer sur l'absorption er la reflectance. modelisation et applications a'la teledetection, Ph.D. thesis, 3rd cycle, 123 pp., Univ. Pierre et Marie Curie, Paris, 1981.

Smith, R. C., and K. S. Baker, The Bio-optical state of ocean waters and remote sensing, *Limnol. Oceanogr.*, *23*, 247–259, 1978a.

Smith, R. C., and K. S. Baker, Optical classification of natural waters, *Limnol. Oceanogr.*, *23*, 260–267, 1978b.

Smith, R. C., and K. S. Baker, Oceanic chlorophyll concentrations as determined by satellite (Nimbus 7 coastal zone color scanner), *Mar. Biol.*, *66*, 269–279, 1982.

Smith, R. C., and W. H. Wilson, Ship and satellite bio-optical research in the California Bight, in *Oceanography From Space*, edited by J. F. R. Gower, pp. 281–294, Plenum, New York, 1981.

Smith, R. C., O. B. Brown, F. E. Hoge, K. S. Baker, R. H. Evans, R. N. Swift, and W. E. Esaias, Multiplatform sampling (ship, aircraft, and satellite) of a Gulf Stream warm core ring, *Appl. Opt.*, *26*, 2068–2081, 1987.

Viollier, M., and B. Sturm, CZCS data analysis in turbid coastal water, *J. Geophys. Res.*, *89*, 4977–4985, 1984.

Walsh, J. J., The Marine Resources Experiment (MAREX), Report of the Ocean Color Science Working Group, 1982, *1983-397-034*, NASA Goddard Space Flight Cent., Greenbelt, Md., 1983.

K. S. Baker, University of California Marine Bio-Optics, Scripps Institution of Oceanography, University of California at San Diego, La Jolla, CA 92093.

J. W. Brown and H. R. Gordon, Department of Physics, University of Miami, Coral Gables, FL 33124.

O. B. Brown and R. H. Evans, Rosentiel School of Marine and Atmospheric Sciences, University of Miami, 4900 Rickenbacker Causeway, Miami, FL 33149.

D. K. Clark, National Environmental Satellite Data Information Service, National Oceanic and Atmospheric Administration, Washington, DC 20233.

R. C. Smith, University of California Marine Bio-Optics, CSL Center for Remote Sensing and Environmental Optics, University of California at Santa Barbara, Santa Barbara, CA 93106.